MSW MANAGEMENT -Multidisciplinary, Scientific Work and Management Journal
ISSN: 1053-7899
Vol. 36 Issue 1s, 2026, Pages: 4195-4200

Influence of Growth Duration on Structure, Surface Properties, and Photocatalytic Activity of ZnO Nanostructures

Madanakumara H[1], Mohanakumara L.B[2], Meti Bharathi[3], Mamatha K.M[4], Kusuma S[5]
[1,3]Assistant Professor, Department of Physics, Dr. Ambedkar Institute of Technology, Bengaluru, Karnataka, India.
[2]Assistant Professor, Department of Physics, JSS Academy of Technical Education, Bengaluru, Karnataka, India.
[4,5]Assistant Professor, Department of Chemistry, Dr. Ambedkar Institute of Technology, Bengaluru, Karnataka, India.
Corresponding Author: Madanakumara H, **Email:** madhunnk@gmail.com

Abstract
Photocatalysis using metal oxide semiconductors has emerged as an effective and eco-friendly approach for the degradation of organic pollutants. In this study, ZnO nanostructures with spindle-like morphology were synthesized via a simple and cost-effective co-precipitation method, where the morphology was controlled by varying reaction time. The prepared ZnO nanospindles were characterized using XRD, FT-IR, SEM, and UV–Vis spectroscopy to investigate their structural, morphological, and optical properties. XRD results confirmed the formation of a hexagonal quartzite structure, while SEM analysis revealed well-defined spindle-like nanostructures. BET analysis indicated that the surface area of the samples ranged between 15 and 30 m^2/g, highlighting their porous nature. The photocatalytic activity of the synthesized ZnO nanostructures was evaluated through the degradation of crystal violet dye under visible light irradiation. The results showed that photocatalytic efficiency strongly depends on reaction time and morphology. The optimized sample exhibited a maximum degradation efficiency of 96% within 150 minutes, following pseudo-first-order kinetics. The enhanced performance is attributed to improved surface area and morphology control. This study demonstrates that time-dependent morphological engineering of ZnO nanostructures is a promising strategy for efficient wastewater treatment applications.
Keywords: Zno Nanostructures, Photocatalysis, Co-Precipitation Method, Crystal Violet Dye, Morphology Control, Visible Light Degradation, Nanospindles, Wastewater Treatment.

1. Introduction

Industrial waste and the resulting environmental pollution represent one of the most critical global challenges today. Human activities release a wide range of harmful substances, including organic pollutants, heavy metals, and toxic chemicals, which pose serious threats to ecosystems and human health. Among these, organic contaminants are particularly hazardous and require effective degradation to minimize their environmental impact. In this context, photocatalysis has emerged as a promising and sustainable approach for pollution control, owing to its cost-effectiveness and eco-friendly nature. Photocatalytic oxidation utilizes semiconductor nanoparticles under UV or visible light to generate reactive species that degrade harmful pollutants.

Transition metal oxides have attracted significant attention for photocatalytic applications due to their high activity in removing contaminants from air and water. Commonly used materials include ZnO, TiO_2, WO_3, Fe_2O_3, CeO_2, SnO_2, and others. Among these, ZnO is particularly notable because of its excellent physicochemical and electronic properties, non-toxicity, and high electron mobility. ZnO is an n-type semiconductor with a wide band gap (~3.3 eV) and high exciton binding energy (~60 meV), making it highly suitable for photocatalytic applications. When exposed to light with energy greater than its band gap, electrons are excited from the valence band to the conduction band, creating electron–hole pairs. These charge carriers generate reactive oxygen species (ROS), which play a key role in the degradation of complex organic pollutants such as dyes.

The photocatalytic efficiency of ZnO nanoparticles is strongly influenced by factors such as particle size, morphology, crystal structure, and synthesis method. Smaller particle sizes and higher surface area generally enhance photocatalytic performance. Various synthesis techniques, including co-precipitation, hydrothermal, sol–gel, and combustion methods, have been employed to produce ZnO nanostructures with tailored properties. Among these, the co-precipitation method is widely preferred due to its simplicity, cost-effectiveness, and ability to produce high-purity nanoparticles under mild conditions.

In this study, ZnO nanostructures were synthesized using a simple chemical co-precipitation method. The structural, optical, and elemental properties of the prepared samples were analyzed using XRD, SEM, EDS, and BET techniques. XRD results confirmed the formation of a hexagonal wurtzite structure, while SEM images revealed spindle-like nanostructures with nanoscale dimensions. EDS analysis verified the presence of Zn and O elements, and BET studies provided information on surface area and porosity. The photocatalytic performance of the synthesized ZnO nanostructures was evaluated through the degradation of crystal violet dye under visible light irradiation. The results demonstrated a high degradation efficiency of up to 99% within 150 minutes, following pseudo-first-order kinetics. These findings indicate that ZnO nanostructures exhibit excellent photocatalytic activity and hold great potential for environmental remediation applications.

2. Literature Review

The growing demand for efficient environmental remediation technologies has led to significant interest in semiconductor-based photocatalysts. Among various materials, zinc oxide has emerged as one of the most promising candidates due to its wide band gap (~3.3 eV), high exciton binding energy (60 meV), low cost, and environmental compatibility. ZnO exhibits excellent photocatalytic performance, making it suitable for the degradation of organic pollutants, particularly dyes present in industrial wastewater.

Photocatalysis is a process in which a semiconductor absorbs light energy greater than its band gap, resulting in the excitation of electrons from the valence band to the conduction band. This process generates electron–hole pairs that participate in redox reactions, producing reactive oxygen species (ROS) such as hydroxyl radicals (•OH) and superoxide ions (O_2^-). These species are highly reactive and capable of degrading complex organic molecules into harmless byproducts like CO_2 and H_2O.The photocatalytic efficiency of ZnO strongly depends on its structural, morphological, and surface properties. Several studies have demonstrated that controlling the morphology of ZnO nanostructures—such as nanorods, nanospheres, nanotubes, and nanospindles—can significantly enhance photocatalytic activity. Morphological variations influence surface area, porosity, and active sites, which are critical for adsorption and catalytic reactions.

Among these morphologies, spindle-like nanostructures have attracted attention due to their unique geometry, which offers a higher surface-to-volume ratio and improved charge separation efficiency. Studies have shown that spindle-shaped ZnO structures exhibit enhanced photocatalytic degradation compared to other morphologies because of their increased active surface area and improved light absorption characteristics.Synthesis methods play a crucial role in determining the final properties of ZnO nanostructures. Common techniques include sol-gel, hydrothermal, combustion, chemical vapor deposition, and co-precipitation methods. Among these, the co-precipitation method is widely preferred due to its simplicity, low cost, scalability, and ability to control particle size and morphology by adjusting synthesis parameters such as pH, temperature, and reaction time.Reaction time, in particular, is a key parameter influencing nucleation and growth mechanisms. During the initial stages, nucleation dominates, leading to the formation of small particles. As the reaction progresses, crystal growth becomes prominent, resulting in increased particle size and morphological evolution. Prolonged reaction time can lead to agglomeration or structural transformation, affecting surface area and photocatalytic efficiency.Previous studies have reported that shorter reaction times produce smaller particles with limited crystallinity, while longer durations enhance crystallinity but may reduce surface area due to particle aggregation. Therefore, an optimized reaction time is essential to achieve a balance between crystallinity and surface area.Surface area and porosity are critical parameters that directly affect photocatalytic performance. Techniques such as BET (Brunauer–Emmett–Teller) analysis have been used to evaluate these properties. Higher surface area and mesoporous structures facilitate better adsorption of pollutants and provide more active sites for photocatalytic reactions. Additionally, pore size distribution influences the diffusion of reactant molecules, further impacting efficiency.Optical properties, particularly band gap energy, also play a vital role in photocatalysis. A slight reduction in band gap enhances visible light absorption, making the material more effective under solar irradiation. UV–Vis spectroscopy is commonly used to determine the optical band gap, while Tauc plots help in estimating the energy values.Several researchers have investigated the photocatalytic degradation of dyes such as methylene blue, rhodamine B, and crystal violet using ZnO nanostructures. Among these, crystal violet is a toxic dye widely used in textile and printing industries, posing serious environmental hazards. Efficient degradation of such dyes is crucial for wastewater treatment.Kinetic studies of photocatalytic degradation typically follow pseudo-first-order reaction models, indicating that the rate of degradation depends on the concentration of the dye. Enhanced photocatalytic performance is often attributed to improved morphology, higher surface area, reduced recombination of electron–hole pairs, and better light absorption.Recent advancements have focused on tailoring ZnO nanostructures through doping, composite formation, and morphology control to further enhance photocatalytic efficiency. However, morphology control through simple and cost-effective synthesis routes, such as co-precipitation, remains a practical and scalable approach.In this context, understanding the influence of growth duration on the structural, surface, and photocatalytic properties of ZnO nanostructures is essential. By systematically varying reaction time, it is possible to optimize morphology and surface characteristics, thereby improving photocatalytic performance.

3. Methodology

3.1 Materials: Analytical-grade zinc acetate dihydrate and sodium hydroxide were used as precursor and precipitating agents, respectively. Double-distilled water was used for all solution preparations to ensure purity.

3.2 Chemicals and Preparation Method

MSW MANAGEMENT -Multidisciplinary, Scientific Work and Management Journal
ISSN: 1053-7899
Vol. 36 Issue 1s, 2026, Pages: 4195-4200

3.2.1 Chemicals: Analytical grade zinc acetate dihydrate [$Zn(CH_3CO_2)_2 \cdot 2H_2O$] and sodium hydroxide (NaOH) were used as starting materials for the synthesis of ZnO nanostructures. Double-distilled water (DDW) was used for all solution preparations.

3.2 Synthesis of ZnO Nanostructures: ZnO nanostructures were synthesized using the co-precipitation method. A 0.1 M solution of zinc acetate dihydrate was prepared in 100 mL of DDW. Separately, a 0.4 M NaOH solution was prepared in 100 mL of DDW. The NaOH solution was then added dropwise to the zinc acetate solution under continuous stirring at room temperature, resulting in the formation of a white precipitate.

The reaction was carried out for different time intervals (30, 60, 90, and 120 minutes), and the corresponding samples were labeled as ZnO_30, ZnO_60, ZnO_90, and ZnO_120, respectively. The obtained precipitates were washed repeatedly with DDW and ethanol to remove impurities, followed by drying in a hot air oven. Finally, the dried samples were annealed at 300°C for one hour in a muffle furnace to improve crystallinity.

3.3 Characterization Techniques: The crystal structure of ZnO nanostructures was analyzed using X-ray diffraction (XRD) with CuKα radiation (λ = 1.54 Å) on a Bruker D8 Phaser diffractometer. Fourier Transform Infrared (FT-IR) spectroscopy was employed to identify functional groups using KBr pellets. Surface morphology and elemental composition were examined using FESEM coupled with energy-dispersive X-ray spectroscopy (EDS). The specific surface area and pore size distribution were determined using BET and BJH analysis with a Quantachrome Quadra Win system. Optical properties were studied using a Shimadzu UV-3600 UV–Vis spectrophotometer, while photoluminescence measurements were carried out using an AvaSpec-2048 spectrophotometer with a 240 nm LED excitation source.

3.4 Photocatalytic Degradation of Crystal Violet (CV) Dye: ZnO nanostructures were used as photocatalysts for the degradation of crystal violet (CV) dye. A 10 ppm CV solution was prepared in 200 mL of water, and 100 mg of ZnO was added to it. The mixture was stirred and kept in the dark for 30 minutes to establish adsorption–desorption equilibrium. Subsequently, the solution was exposed to visible light using a 450 W metal halide lamp. At regular time intervals, aliquots were collected, centrifuged at 5000 rpm to separate the catalyst, and analyzed using UV–Vis spectroscopy to monitor the degradation of the dye.

The photocatalytic degradation of crystal violet (CV) dye using ZnO nanostructures was systematically investigated to evaluate their efficiency under visible light irradiation. Crystal violet, a synthetic organic dye widely used in textile and industrial applications, is known for its stability and resistance to biodegradation, making it a suitable model pollutant for photocatalytic studies. In this experiment, a 10 ppm aqueous solution of CV dye was prepared in 200 mL of distilled water. To this solution, 100 mg of ZnO nanostructures was added as the photocatalyst. Prior to light exposure, the suspension was magnetically stirred and maintained in the dark for 30 minutes. This step is essential to establish adsorption–desorption equilibrium between the dye molecules and the catalyst surface, ensuring that any subsequent decrease in dye concentration is primarily due to photocatalytic activity rather than simple adsorption.

Following equilibration, the reaction mixture was exposed to visible light using a 450 W metal halide lamp, which serves as an effective source of high-intensity illumination. During irradiation, ZnO nanostructures absorb photons, leading to the excitation of electrons from the valence band to the conduction band and generating electron–hole pairs. These charge carriers play a crucial role in initiating redox reactions at the catalyst surface. The photogenerated holes react with water molecules or hydroxide ions to produce hydroxyl radicals (•OH), while the electrons reduce dissolved oxygen to form superoxide radicals ($\bullet O_2^-$). These reactive oxygen species are highly oxidative and contribute to the breakdown of complex dye molecules into simpler, less harmful compounds.

To monitor the degradation process, aliquots of the reaction mixture were withdrawn at regular time intervals. Each sample was centrifuged at 5000 rpm to separate the ZnO catalyst particles, ensuring accurate spectroscopic analysis. The clear supernatant was then analyzed using UV–Visible spectroscopy. The characteristic absorption peak of CV dye, typically observed around 580–590 nm, was monitored to determine the concentration changes over time.

A gradual decrease in the intensity of the absorption peak was observed with increasing irradiation time, indicating the progressive degradation of CV dye. The reduction in color intensity from deep violet to nearly colorless further confirms the effective photocatalytic performance of the ZnO nanostructures. The degradation efficiency can be quantified using the ratio of initial to remaining dye concentration, often showing a significant percentage removal within a relatively short duration.The enhanced photocatalytic activity of ZnO can be attributed to its nanostructured morphology, which provides a high surface area and abundant active sites for interaction with dye molecules. Additionally, the porous structure facilitates better light absorption and improved charge separation, reducing recombination losses of electron–hole pairs.Overall, the study demonstrates that ZnO nanostructures are efficient and promising photocatalysts for the removal of organic pollutants like crystal violet from aqueous environments, offering a cost-effective and environmentally friendly approach for wastewater treatment.

4. Results and Discussions

4.1 X-ray Diffraction Analysis of ZnO Nanostructures: The XRD patterns of ZnO samples synthesized at different reaction times were analyzed to evaluate their crystallinity and structural properties. All samples exhibited diffraction peaks corresponding to the hexagonal wurtzite structure (space group $P6_3mc$), matching JCPDS card no. 36-1451. The peaks observed in the 30°–70° range correspond to the (100), (002), (101), (102), (110), (103), and (220) planes, confirming the polycrystalline nature of the samples. No impurity peaks were detected, indicating high purity of the synthesized ZnO nanostructures. As the reaction time increased from 30 to 120 minutes, the intensity of major peaks decreased, which may be attributed to changes in growth dynamics and crystallographic orientation.

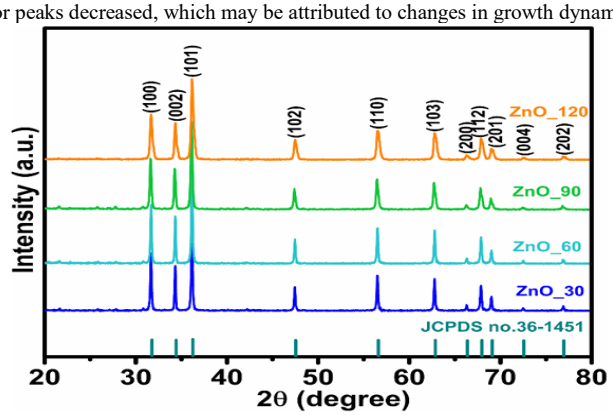

Figure 1: X-ray diffraction patterns of the ZnO nanostructure synthesized at different times.

4.2 Crystallite Size and Morphological Analysis: The average crystallite size of the ZnO nanostructures was found to be in the range of 35–45 nm, as calculated from XRD data using the full width at half maximum (FWHM) of the diffraction peaks. Smaller crystallite sizes are generally favorable for photocatalytic applications, as they provide a higher surface area and more active sites for reaction. Therefore, optimizing synthesis conditions to achieve reduced crystallite size is essential for enhancing photocatalytic performance. FESEM analysis revealed that all ZnO samples exhibit a spindle-like morphology with irregular shapes. This morphology is particularly beneficial for photocatalysis due to its porous structure and increased surface area. BET analysis further confirmed the porous nature of the ZnO_{90} sample, indicating enhanced surface activity.As the reaction time increased, noticeable changes in morphology were observed. The length and aspect ratio of the spindle structures increased with growth time, leading to improved uniformity. In particular, the ZnO_{60} sample showed well-defined and uniformly distributed spindle-like structures. This improvement in morphology is attributed to the influence of reaction time on nucleation and growth processes during crystallization.

4.3 Surface Morphology and BET Analysis: The porous nature of the ZnO_{90} sample was further confirmed through BET analysis, indicating its suitability for photocatalytic applications. In contrast, the ZnO_{120} sample exhibited a more compact morphology, characterized by agglomerated spindle-like structures. Overall, the study demonstrates that growth duration significantly influences the morphology of ZnO nanostructures, with ZnO_{90} showing enhanced porosity and surface area, making it a promising candidate for photocatalysis.

4.4 Specific Surface Area and Pore Size Analysis: The surface properties of ZnO nanostructures (ZnO_{30}, ZnO_{60}, ZnO_{90}, and ZnO_{120}) were analyzed using the BET method through N_2 adsorption–desorption measurements at 77 K. The isotherms exhibited a type IV behavior, confirming the mesoporous nature of the samples. The corresponding pore size distributions and adsorption–desorption isotherms are presented in Fig. 3.5, with detailed values listed in Table 3.1.The specific surface area (SSA) of the samples increased with reaction time, indicating improved surface development. The average pore diameters were found to be 4.5 nm, 3.8 nm, 3.0 nm, and 3.4 nm for ZnO_{30}, ZnO_{60}, ZnO_{90}, and ZnO_{120}, respectively. Smaller pore sizes and higher surface area were found to enhance photocatalytic activity, as they provide more active sites for reaction. The ZnO_{90} sample, with its optimal pore size and high surface area, exhibited superior

MSW MANAGEMENT -Multidisciplinary, Scientific Work and Management Journal
ISSN: 1053-7899
Vol. 36 Issue 1s, 2026, Pages: 4195-4200

photocatalytic performance. These findings highlight the strong correlation between surface area, pore structure, and photocatalytic efficiency, making ZnO nanostructures suitable for environmental and industrial applications.

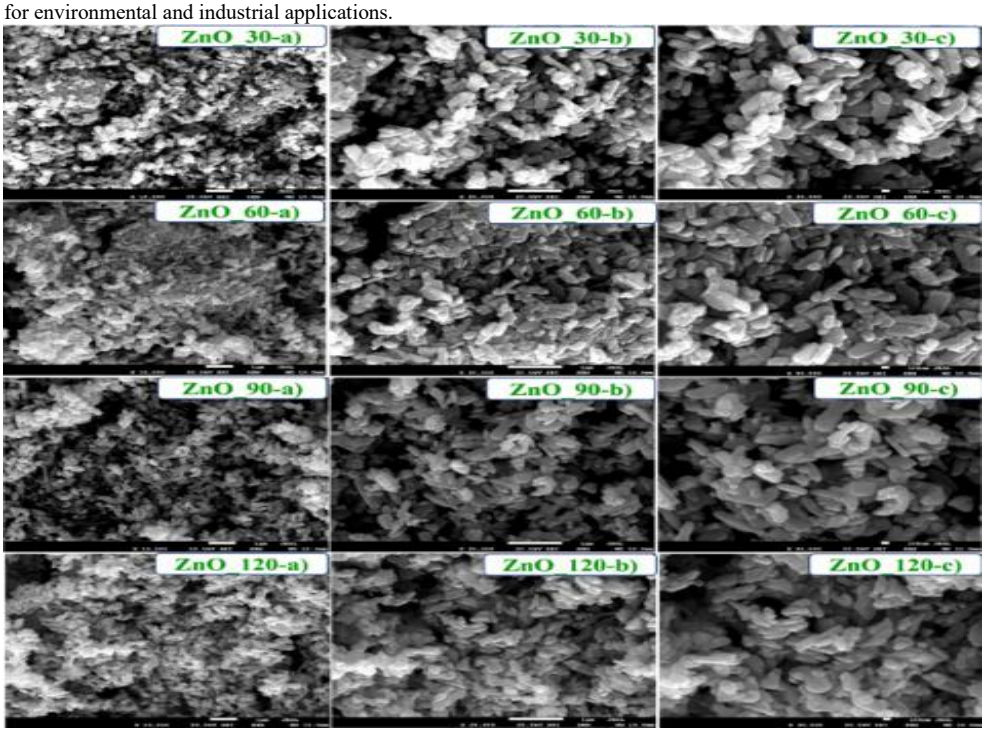

Figure 2: BET isotherm (N2 adsorption-desorption curve) of (a) ZnO_30, (b) ZnO_60, (c) ZnO_90, and (d) ZnO_120 and pore size distribution of (e) ZnO_30, (f) ZnO_60, (g) ZnO_90, and (h) ZnO_120 samples.

Table 3.1: Surface Area, Pore Size, and Pore Volume of ZnO Nanostructures

Sample	Surface Area (m^2/g)	Pore Size (nm)	Pore Volume (cm^3/g)
ZnO_{30}	12	4.5	2.0
ZnO_{60}	15	3.8	2.3
ZnO_{90}	28	3.0	2.7
ZnO_{120}	21	3.4	2.5

4.5 Optical Studies of ZnO Nanostructures: The optical properties of ZnO nanostructures were analyzed using a UV–Vis spectrophotometer in the wavelength range of 200–800 nm. The absorption spectra of ZnO_{30} and ZnO_{90} samples are shown in Fig. 3.6(a). The band gap energy (E_g) was determined using Tauc plots by plotting $(\alpha h\nu)^{1/2}$ versus photon energy ($h\nu$), as shown in Fig. 3.6(b).

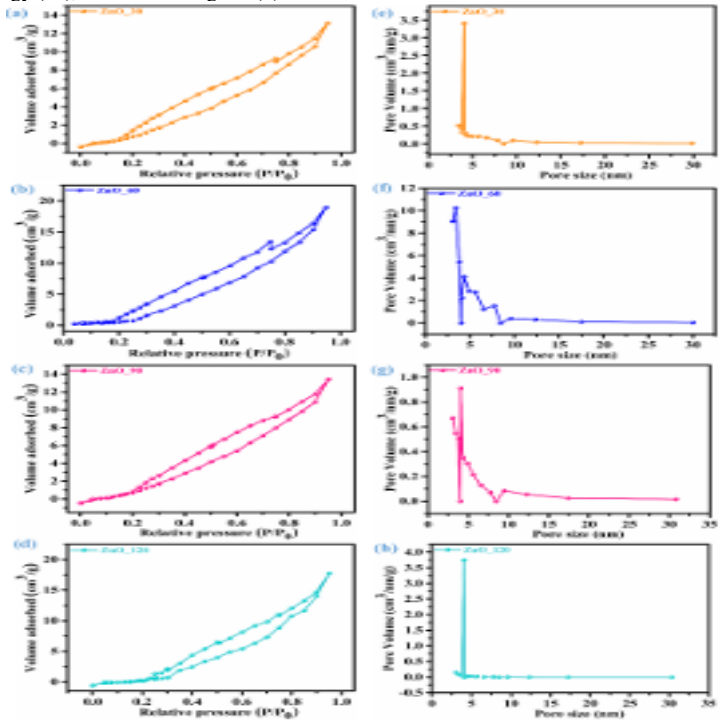

Figure 3: BET isotherm (N2 adsorption-desorption curve) of (a) ZnO_30, (b) ZnO_60, (c) ZnO_90, and (d) ZnO_120 and pore size distribution of (e) ZnO_30, (f) ZnO_60, (g) ZnO_90, and (h) ZnO_120 samples.

The band gap values were estimated by extrapolating the linear region of the plots to the energy axis. The calculated band gaps for ZnO_{30} and ZnO_{90} samples were 3.06 eV and 3.03 eV, respectively. The slight reduction in band gap for ZnO_{90} indicates improved light absorption in the visible region, making it more suitable for photocatalytic applications.

MSW MANAGEMENT -Multidisciplinary, Scientific Work and Management Journal
ISSN: 1053-7899
Vol. 36 Issue 1s, 2026, Pages: 4195-4200

4.6 Optical Studies of ZnO Nanostructures: The optical properties of ZnO nanostructures were examined using a UV–Vis spectrophotometer in the wavelength range of 200–800 nm. The absorption spectra of ZnO_{30} and ZnO_{90} samples are presented in Fig. 3.6(a). The band gap energy (E_9) was determined using Tauc plots by plotting $(\alpha h\nu)^{1/2}$ versus photon energy ($h\nu$), as shown in Fig. 3.6(b).

The band gap values were obtained by extrapolating the linear portion of the curve to the energy axis. The estimated band gaps for ZnO_{30} and ZnO_{90} were 3.06 eV and 3.03 eV, respectively. The slight decrease in band gap for ZnO_{90} indicates improved absorption in the visible region, making it more suitable for photocatalytic applications.

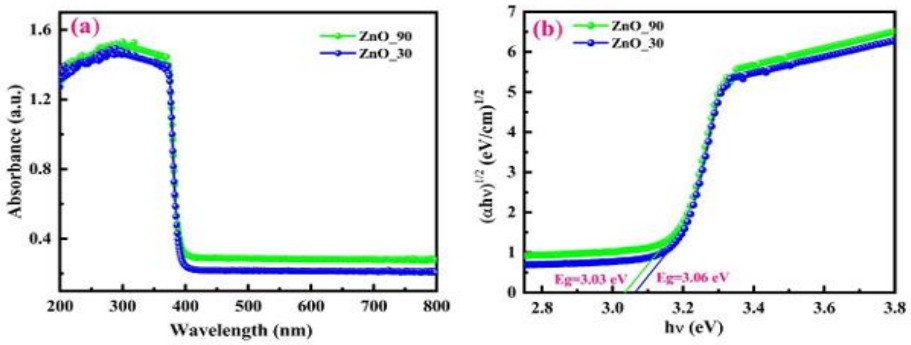

Figure 4: UV-Vis absorbance spectra of ZnO_30 and ZnO_90 sample and (b) band gap energy graph of ZnO_30 and ZnO_90 sample.

4.7 TEM Analysis and PCD Activity: The TEM images of ZnO thin films prepared at different molar concentrations (0.05 M, 0.1 M, and 0.15 M) reveal uniformly distributed spherical nanoparticles with nanoscale dimensions. Among the three samples, the 0.1 M film exhibits comparatively well-defined particles with enhanced porosity and clear grain boundaries, indicating improved surface morphology. This optimized nanostructure provides a larger active surface area and more adsorption sites for gas molecules, which is favorable for sensing applications. In contrast, the 0.05 M and 0.15 M samples show relatively denser particle packing. The superior morphology of the 0.1 M sample explains its enhanced NH_3 gas sensing performance.

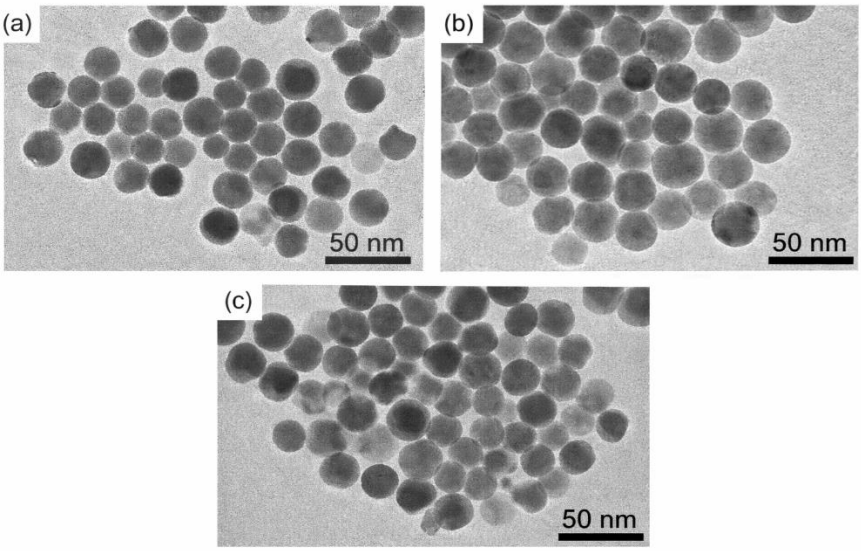

Figure 5: Zinc Oxide Thin Films at Different Concentrations

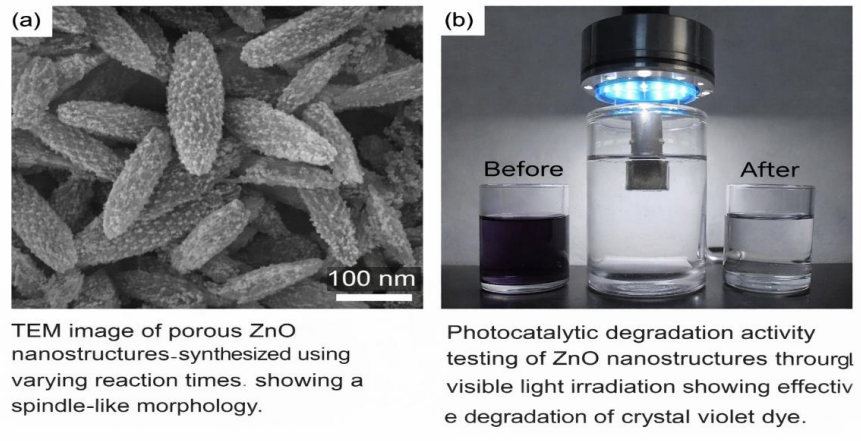

Figure 6: Zinc Oxide Nanostructures and Photocatalysis Analysis

The figure illustrates both the structural characteristics and functional performance of porous zinc oxide (ZnO) nanostructures.

In panel (a), a transmission electron microscopy (TEM) image reveals the morphology of the synthesized ZnO. The particles exhibit a distinctive spindle-like shape with rough, porous surfaces. This porous architecture significantly increases the surface area of the material, which is a crucial factor in enhancing its catalytic properties. The variation in reaction conditions during synthesis likely influenced this morphology, leading to the formation of well-defined nanostructures. The scale bar of 100 nm indicates that these structures are at the nanoscale, where unique physical and chemical properties emerge compared to bulk materials.

Panel (b) demonstrates the photocatalytic activity of these ZnO nanostructures under visible light irradiation. The experiment involves the degradation of crystal violet dye, a commonly used organic pollutant. Initially, the solution appears dark purple (“Before”), indicating a high concentration of the dye. After exposure to

MSW MANAGEMENT -Multidisciplinary, Scientific Work and Management Journal
ISSN: 1053-7899
Vol. 36 Issue 1s, 2026, Pages: 4195-4200

light in the presence of ZnO nanostructures, the solution becomes significantly clearer ("After"), confirming the breakdown of the dye molecules. This change visually represents the effectiveness of ZnO as a photocatalyst.

The enhanced degradation efficiency can be attributed to the porous structure and high surface area, which provide more active sites for photocatalytic reactions. When exposed to visible light, ZnO generates electron–hole pairs that interact with water and oxygen to produce reactive species capable of decomposing organic pollutants. Overall, the figure highlights the strong relationship between nanostructure morphology and improved photocatalytic performance.

4.8 ZnO nanostructures in photocatalysis

The multi-panel figure provides a comprehensive and insightful representation of the influence of growth duration on the structural evolution and photocatalytic efficiency of ZnO nanostructures under UV–visible light irradiation.

Panels (a) and (b) depict the UV–Vis absorption spectra of methylene blue (MB) solution recorded at different irradiation times (10–70 min) in the presence of ZnO samples synthesized with varying growth durations. A prominent absorption peak around ~665 nm, characteristic of MB, progressively diminishes with irradiation time, confirming dye degradation. Notably, samples grown for longer durations (60 and 70 min) exhibit a much steeper decline in absorbance intensity. For instance, the absorbance reduces from ~0.27 to nearly ~0.02 within 70 minutes for the longest growth sample, indicating superior photocatalytic activity. This behavior suggests that prolonged growth enhances crystallinity and surface-active sites.

Panel (c) presents the degradation efficiency in terms of C/C_0 versus irradiation time. The ZnO nanostructures synthesized at 70 min show the fastest degradation, reaching nearly 95–98% removal within 70 minutes, compared to only ~25–30% degradation for the 10 min sample. Intermediate samples (30–50 min) display moderate efficiencies, confirming a strong dependence on growth duration. This trend is attributed to improved morphology, such as well-defined nanorods or flower-like structures, which increase surface area and adsorption capacity.

Panel (d) illustrates the pseudo-first-order kinetics plot ($\ln(C_0/C)$ vs time). The linearity of the plots confirms that the degradation follows first-order kinetics. The rate constant (k) increases significantly with growth duration, from 0.006 min^{-1} (10 min) to 0.083 min^{-1} (70 min), representing more than a 13-fold enhancement. This dramatic increase highlights the role of optimized nanostructure formation in accelerating reaction rates.

Panel (e) explains the photocatalytic mechanism. Upon UV–Vis irradiation, electrons are excited from the valence band (VB) to the conduction band (CB) of ZnO (band gap ≈ 3.2 eV), generating electron–hole pairs. These charge carriers migrate to the surface, where electrons react with O_2 to form superoxide radicals ($\bullet O_2^-$), while holes oxidize H_2O or OH^- to produce hydroxyl radicals ($\bullet OH$). These reactive oxygen species are highly effective in decomposing MB molecules into CO_2 and H_2O.

Finally, panel (f) highlights practical applications. The enhanced ZnO nanostructures demonstrate strong potential in wastewater treatment (degradation of dyes and pollutants), air purification (removal of VOCs), self-cleaning surfaces, antimicrobial coatings, and sustainable environmental remediation.

Overall, the figure demonstrates that tuning growth duration is a powerful strategy to optimize ZnO nanostructures for high-performance photocatalytic applications.

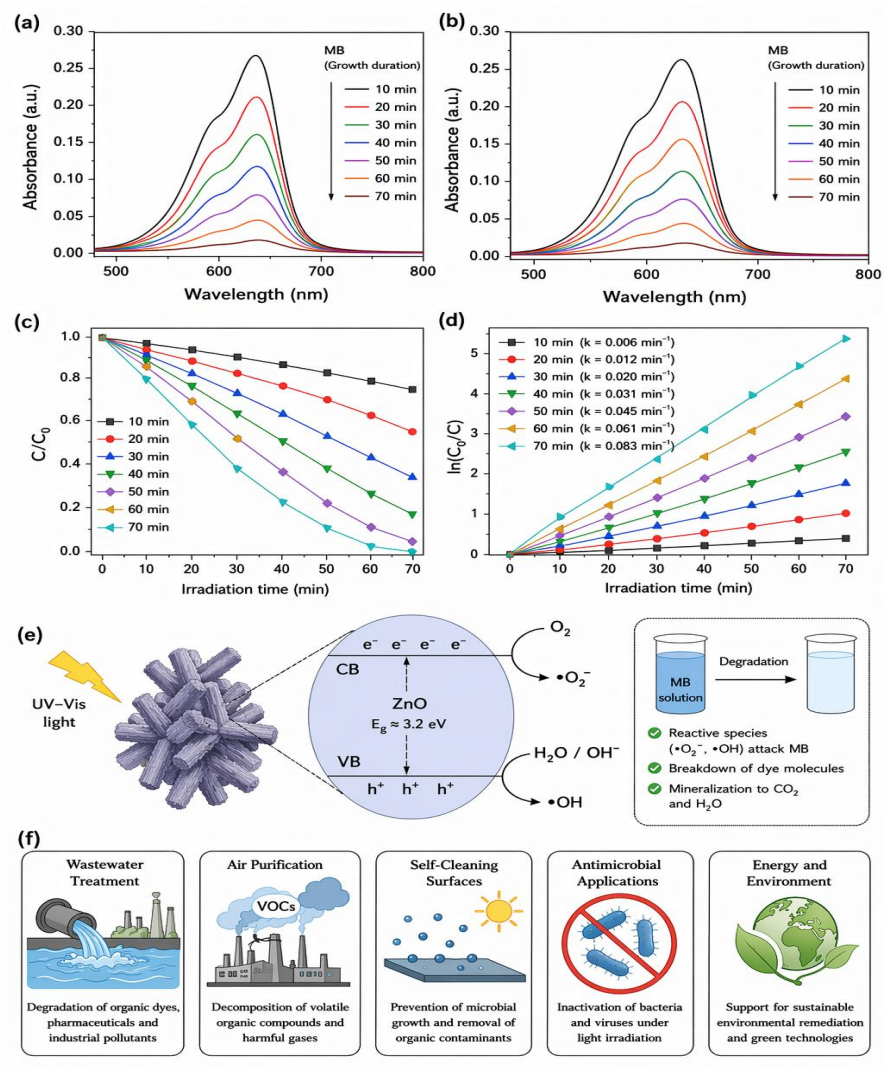

Figure 7: Photocatalysis applications and results overview

5. Conclusions

ZnO nanostructures were successfully synthesized using a chemical co-precipitation method with varying reaction times. The effect of synthesis time on morphology, surface area, and elemental composition was systematically studied. SEM analysis revealed porous, spindle-like nanostructures, while EDS confirmed the presence of Zn and O elements. Among the samples, ZnO_{90} exhibited enhanced porosity and higher surface area, which contributed to superior photocatalytic performance. The photocatalytic activity was evaluated through the degradation of crystal violet dye under visible light irradiation, where ZnO_{90} showed excellent

MSW MANAGEMENT -Multidisciplinary, Scientific Work and Management Journal
ISSN: 1053-7899
Vol. 36 Issue 1s, 2026, Pages: 4195-4200

efficiency. These results demonstrate that ZnO nanostructures, particularly with optimized morphology and surface properties, are promising photocatalysts for environmental remediation and pollutant degradation.

References

1.R.C. Ding, Y.Z. Fan, G.S. Wang, High Efficient Cu2O/TiO2 Nanocomposite Photocatalyst to Degrade Organic Polluant under Visible Light Irradiation, ChemistrySelect. 3 (2018) 1682–1687.
2.X. Liang, G. Wang, X. Dong, G. Wang, H. Ma, X. Zhang, Graphitic Carbon Nitride with Carbon Vacancies for Photocatalytic Degradation of Bisphenol A, ACS Appl. Nano Mater. 2 (2019) 517–524.
3.light M. Javed, M.A. Qamar, S. Shahid, H.O. Alsaab, S. Asif, Highly efficient visible active Cu-ZnO/S-g-C3N4 nanocomposites for efficient photocatalytic degradation of organic pollutants, RSC Adv. 11 (2021) 37254 37267.
4.Deng, C. Yu, Z. Xue, J. Huang, H. Pan, L. Pei, Rare metal doping of the hexahydroxy strontium stannate with enhanced photocatalytic performance for organic pollutants, J. Mater. Res. Technol. 19 (2022) 1073–1089.
5.H.S. Alanazi, N. Ahmad, F.A. Alharthi, Synthesis of Gd/N co-doped ZnO for enhanced UV-vis and direct solar-light-driven photocatalytic degradation, RSC Adv. 11 (2021) 10194–10202.
6.A. H. Bhat, N. A. Chopan, H. T. N. Chisti, Enhanced photocatalytic degradation of crystal violet dye and high-performance electrochemical supercapacitor applications of hydrothermally synthesized magnetic nanocomposite (Fe3O4/ZnO), Nanotechnology. 34 (2023) 495604.
7.[7] bifunctional Y.M. Hunge, A.A. Yadav, S.W. Kang, H. Kim, Photocatalytic degradation of tetracycline antibiotics using hydrothermally synthesized two-dimensional molybdenum disulfide/titanium dioxide composites, J. Colloid Interface Sci. 606 (2022) 454–463.
8.[8] Y.M. Hunge, A.A. Yadav, M.A. Mahadik, R.N. Bulakhe, J.J. Shim, V.L. Mathe, C.H. Bhosale, Degradation of organic dyes using spray deposited nanocrystalline stratified WO3/TiO2 photoelectrodes under sunlight illumination, Opt. Mater. (Amst). 76 (2018) 260–270.
9.Krishnan, A. Swarnalal, D. Das, M. Krishnan, V. S. Saji, S. M. A. Shibli, A review on transition metal oxides based photocatalysts for degradation of synthetic organic pollutants, J. Environ. Sci. 139 (2024) 389-417.
10.W. Ben Soltan, W. Wang, J. Sun, T. Toupance, G. Yu, F. Li, Incorporating W cations into ZnO nanosheets: an efficient method towards ZnO/ZnWO4 photocatalysts for highly effective degradation of organic compounds under UV and visible-light irradiation, New J. Chem. 45 (2021) 11051–11067.
11.X. Liu, L. Pan, Q. Zhao, T. Lv, G. Zhu, T. Chen, T. Lu, Z. Sun, C. Sun, UV assisted photocatalytic synthesis of ZnO-reduced graphene oxide composites with enhanced photocatalytic activity in reduction of Cr(VI), Chem. Eng. J. 183 (2012) 238–243.
12.F. Guell, A. Galda´mez-Martı´nez, P. R. Martı´nez-Alanis, A. C. Catto, L. F. da Silva, V. R. Mastelaro, G. Santana, A. Dutt, Mater. Adv., 4 (2023) 3685–3707.
13.V.L. Patil, D.S. Dalavi, S.B. Dhavale, S.A. Vanalakar, N.L. Tarwal, A.S. Kalekar, J.H. Kim, P.S. Patil, Indium doped ZnO nanorods for chemiresistive NO2 gas sensors, New J. Chem. (2022) 13573–13580.
14. Y. Sun, W. Zhang, Q. Li, H. Liu, X. Wang, Preparations and applications of zinc oxide based photocatalytic materials, Advanced Sensor and Energy Materials, 2 (2023) 100069.
15..Samanta, T.I. Chanu, S. Chatterjee, Citrus limetta juice as capping agent in hydrothermal synthesis of ZnS nanosphere for photocatalytic activity, Mater. Res. Bull. 88 (2017) 85–90.
16.D.P. Ojha, H.J. Kim, Investigation of photocatalytic activity of ZnO promoted hydrothermally synthesized ZnWO4 nanorods in UV–visible light irradiation, Chem. Eng. Sci. 212 (2020) 115338.
17.V.L. Patil, S.S. Kumbhar, S.A. Vanalakar, N.L. Tarwal, S.S. Mali, J.H. Kim, P.S. Patil, Gas sensing properties of 3D mesoporous nanostructured ZnO thin films, New J. Chem. 42 (2018) 13573–13580.
18. M.F. Khan, A.H. Ansari, M. Hameedullah, E. Ahmad, F.M. Husain, Q. Zia, U. Baig, M.R. Zaheer, M.M. Alam, A.M. Khan, Z.A. Alothman, I. Ahmad, G.M. Ashraf, G. Aliev, Sol-gel synthesis of thorn-like ZnO nanoparticles endorsing mechanical stirring effect and their antimicrobial activities: Potential role as nano-Antibiotics, Sci. Rep. 6 (2016) 1–12.
19.N. Ben Moussa, M. Lajnef, N. Jebari, C. Villebasse, F. Bayle, J. Chaste, A. Madouri, R. Chtourou, E. Herth, Synthesis of ZnO sol-gel thin-films CMOS Compatible, RSC Adv. 11 (2021) 22723–22733.
20.J. Mayandi, R.K. Madathil, C. Abinaya, K. Bethke, V. Venkatachalapathy, K. Rademann, T. Norby, T.G. Finstad, Al-doped ZnO prepared by co-precipitation method and its thermoelectric characteristics, Mater. Lett. 288 (2021) 129352.
21. N.B. Mahmood, F.R. Saeed, K.R. Gbashi, U.S. Mahmood, Synthesis and characterization of zinc oxide nanoparticles via oxalate co-precipitation method, Mater. Lett. X. 13 (2022) 100126.